NANO MICRO small

Supporting Information

for *Small,* DOI: 10.1002/smll.202104761

Rapid Synthesis of High-Entropy Oxide Microparticles

*Qi Dong, Min Hong, Jinlong Gao, Tangyuan Li, Mingjin Cui, Shuke Li, Haiyu Qiao, Alexandra H. Brozena, Yonggang Yao, Xizheng Wang, Gang Chen, Jian Luo, and Liangbing Hu**

Supporting Information for

Rapid Synthesis of High-Entropy Oxide Microparticles

Qi Dong,[1,a] Min Hong,[1,a] Jinlong Gao,[1,a] Tangyuan Li,[1] Mingjin Cui,[1] Shuke Li,[1] Haiyu Qiao,[1] Alexandra H. Brozena,[1] Yonggang Yao,[1] Xizheng Wang,[1] Gang Chen,[1] Jian Luo,[2] Liangbing Hu[1,3*]

[1]Department of Materials Science and Engineering, University of Maryland, College Park, Maryland 20742, United States

[2]Department of NanoEngineering, University of California, San Diego, La Jolla, California 92093, United States

[3]Center for Materials Innovation, University of Maryland, College Park, Maryland 20742, United States

[a]These authors contributed equally.

[*]binghu@umd.edu

Methods

Starting materials

Metal nitrate precurosrs, including $Mn(NO_3)_2 \cdot xH_2O$, $Fe(NO_3)_3 \cdot 9H_2O$, $Co(NO_3)_2 \cdot 6H_2O$, $Ni(NO_3)_2 \cdot 6H_2O$, $Cu(NO_3)_2 \cdot 3H_2O$, $Zn(NO_3)_2 \cdot 6H_2O$, $Mg(NO_3)_2 \cdot 6H_2O$, $Cr(NO_3)_3 \cdot 9H_2O$, $Ca(NO_3)_2 \cdot 4H_2O$, and $Al(NO_3)_3 \cdot 9H_2O$ of at least ACS reagent grade were purchased from Sigma-Aldrich. The precursors were all used as received without further purification or grinding. 1-Methyl-2-pyrrolidinone (≥ 99.0%), poly(vinylidene fluoride) (average M_w ~534,000 by GPC, powder), NiO (nanopowder), and ZnO (nanopowder) were also obtained from Sigma-Aldrich. For the Li-ion battery test, the electrolyte composed of 1 M $LiPF_6$ in ethylene carbonate and diethyl carbonate (EC/DEC=50/50 (v/v)) was obtained from Gotion. Ketjen Black was obtained from Cabot Corporation as a conductive substance for electrode preparation. Lithium ribbon (≥ 99.9%, trace metals basis, 0.38 mm) was purchased from Sigma-Aldrich. The $LiFePO_4$ cathode was obtained from MTI Corp. Carbon paper (Freudenburg H23) was obtained from the Fuel Cell Store. Multi-purpose copper sheets (99.9%, 0.002" thickness) and wires (99.9%) were obtained from McMaster Carr for electrical connections.

Temperature measurement

The temperature of the Joule-heated carbon paper was measured using a previously established technique.[1] In this approach, a high-speed camera (Vision Research Phantom Miro M110) is used to record the color ratio pyrometry of the sample at a rate of 1000 frames/s. The profile of the heating temperature as a function of time was calculated based on the gray-body assumption and Planck's law.[2,3] MATLAB was further applied to deconvolute the color information for each pixel to estimate the temperature with an error threshold of ~110 K.[3]

Spectroscopic and microscopic characterization

A PANalytical X'Pert Pro diffractometer with a Cu Kα source was used for the XRD measurements. A Thermo Scientific K-Alpha+ instrument with an Al X-ray source (1486.7 eV photon energy) was applied for XPS. SEM-EDX was conducted using Tescan GAIA FEG and Tescan XEIA FEG instruments with 5 kV or 10 kV accelerating voltages. The elemental maps of the senary HEO synthesized by the high-temperature rapid heating approach were collected using STEM-EDX on a JEM 2100 FEG for better resolution. The elemental maps of the other compositions were collected by SEM-EDX.

Reactor setup and synthesis protocols

A VOLTEQ power source (model HY7520EX) was used for Joule heating the carbon paper. A ribbon of flexible carbon paper (~1.5 cm × 6 cm) was connected with copper wires on each end. The power source had an adjustable input power, which was applied to the carbon paper to generate Joule heating and to reach the desired temperature by tuning the input voltage. The metal nitrate precursors in equal molar ratio were placed on the folded carbon paper prior to turning on the electrical power. The synthesis can be conducted under air or an atmosphere with lower oxygen partial pressure, with the former being more destructive to the carbon paper but more efficient in creating the HEO particles. Note that the carbon paper substrate is sacrificed during the synthetic process. During electrical Joule heating, the exhaust was ventilated or absorbed by a wet $NaOH/Ca(OH)_2$ mixture. The synthesis based on electrical Joule heating at ~1500 K typically takes ~15 s for gram-scale production. The reaction was considered complete when no gaseous products

were further generated and the solid mixture was visually homogeneous. Slightly longer heating durations (*e.g.*, an additional 10 s) may be used to ensure good product quality. After turning off the electrical power, the sample product was collected by scraping off the HEO powder from the carbon heater for further characterization and analysis.

In a typical process to synthesize senary HEO, ~1.5 g nitrate precursors including $Mn(NO_3)_2 \cdot xH_2O$, $Fe(NO_3)_3 \cdot 9H_2O$, $Co(NO_3)_2 \cdot 6H_2O$, $Ni(NO_3)_2 \cdot 6H_2O$, $Cu(NO_3)_2 \cdot 3H_2O$, $Zn(NO_3)_2 \cdot 6H_2O$ were mixed in equal molar ratio in a glass vial and then transfered onto a folded carbon paper (as shown in Fig. 1B and Fig. 2A; ~2 cm in width, ~5 cm in length). Due to the hydration of the precursors, their mixture often appears as a pile of wet paste that can be used without further spreading. The carbon paper was connected with electrical wires on the two ends and Joule heated in open air (1 atm; 21 vol% O_2) at ~1500 K for ~15 s. The voltage and current input depend on the type and geometry of the carbon paper, which are typically <20 V and <15 A, respectively. After reaction, the product appears as dark powders that can be scratched off from the carbon heater.

Li-ion battery test

The senary HEO powder and unary oxide powders were investigated as anode active materials (80 wt%). The anode active material was manually mixed with Ketjen Black (10 wt%) and grounded for 30 min. 10 wt% of poly(vinylidene fluoride) was then added as binder. The mixture was further milled for another 30 min in a mortar. The final slurry was coated onto a Cu foil using a doctor blade. CR2032 coin cells were used in this study for both half-cell and full-cell analyses. 75 μL 1 M $LiPF_6$ in EC:DEC was applied as the electrolyte for both half-cell and full-cell tests. Polypropylene membrane was used as separator for both half-cell and full-cell tests. The cells were all tested on a Neware battery analyzer at 298 K. Half-cells were assembled using Li metal foil as the counter electrode (0.38 mm, > 20 times excess capacity). Half-cell charging/discharging tests were conducted using a series of current densities with a voltage window from 0.01 V to 3 V. Full-cells were assembled using the senary HEO as the anode and $LiFePO_4$ (MTI) as the cathode. A pre-lithiation step was conducted for the senary HEO anode prior to the full cell assembly. As the Coulombic efficiency of the senary HEO is characterized in half-cells, the purpose of full-cell tests is to observe the compatibility of the senary HEO with commercial cathode materials. For full-cells, the senary HEO anode was used with 2 times excess capacity. In a typical process, half-cells made of HEO and Li were cycled at C/20 for three times. The pre-cycled senary HEO was extracted and used for the full-cell test. The full-cell charging/discharging test was conducted at C/5 with a voltage window from 0.8 V to 3.6 V. The capacity, Coulombic efficiency and rate performance reported in this work have been confirmed with at least 3 cells.

Electrochemical testing for the oxygen evolution reaction

The quinary HEO (*i.e.*, $(Fe,Co,Ni,Mn,Zn)O_x$) powder was grounded with Vulcan XC72 carbon (*e.g.*, 4 mg HEO and 3 mg carbon) in a Nafion (0.5 wt%) isopropanol solution (1:3 in volume). The mixture was drop cast on a glassy carbon electrode yielding a loading of ~0.7 mg/cm^2. A AgCl/Ag reference electrode and a Pt mesh counter electrode were used together with the loaded glassy carbon working electrode. 1.0 M KOH solution was used as the electrolyte. Linear sweeping voltammetry (LSV) was conducted using a scan rate of 1 mV/s from the open circuit potential to 2.0 V *vs.* RHE in a rotating disc electrode setup. Tafel analysis was conducted based on the measured LSV curves.

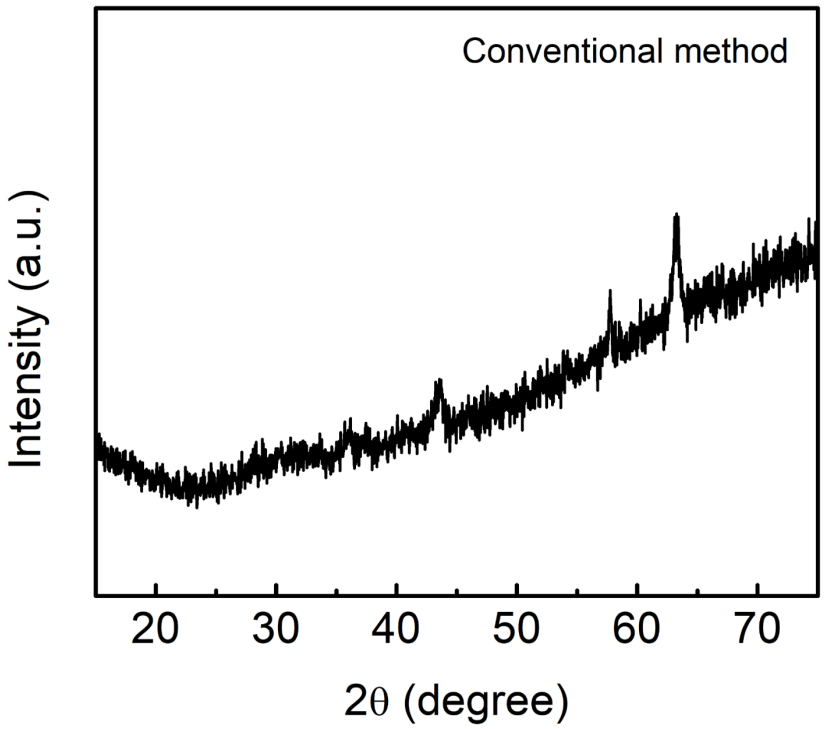

Figure S1. X-ray diffraction pattern of the senary spinel oxide (*i.e.*, $(Mn,Fe,Co,Ni,Cu,Zn)_3O_{4-x}$) synthesized by the conventional furnace heating method at 1100 K for 2 hours.

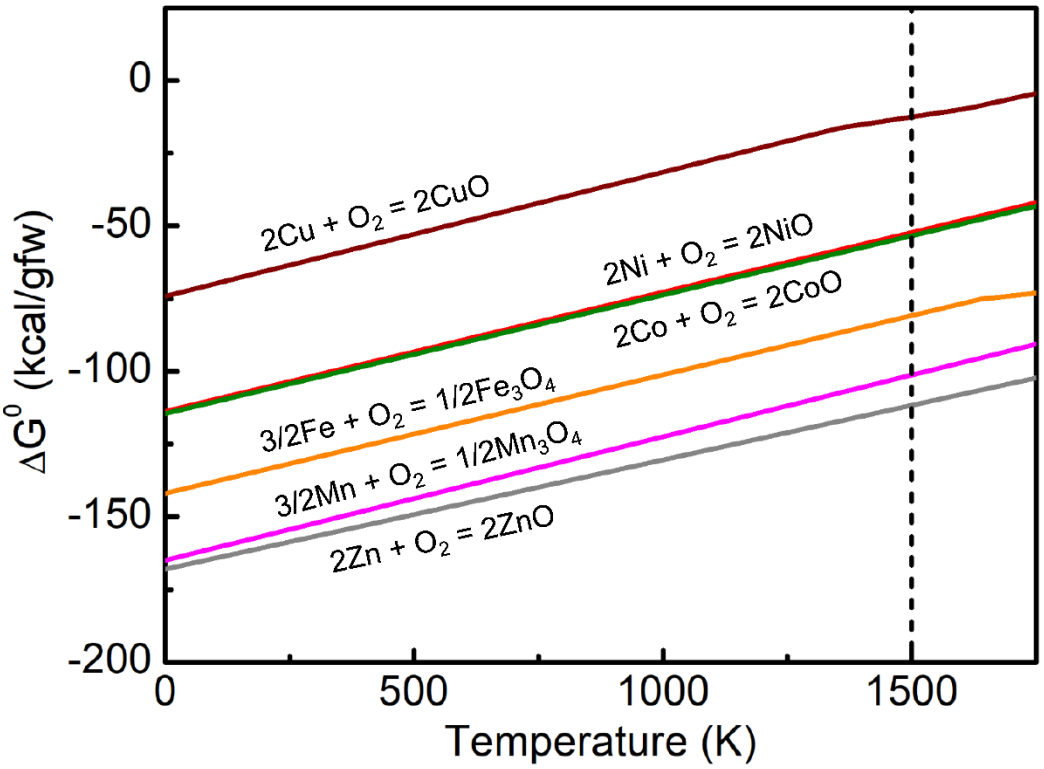

Figure S2. Ellingham diagram showing the trend of oxidation potentials: Zn > Mn > Fe > Co > Ni > Cu.[4]

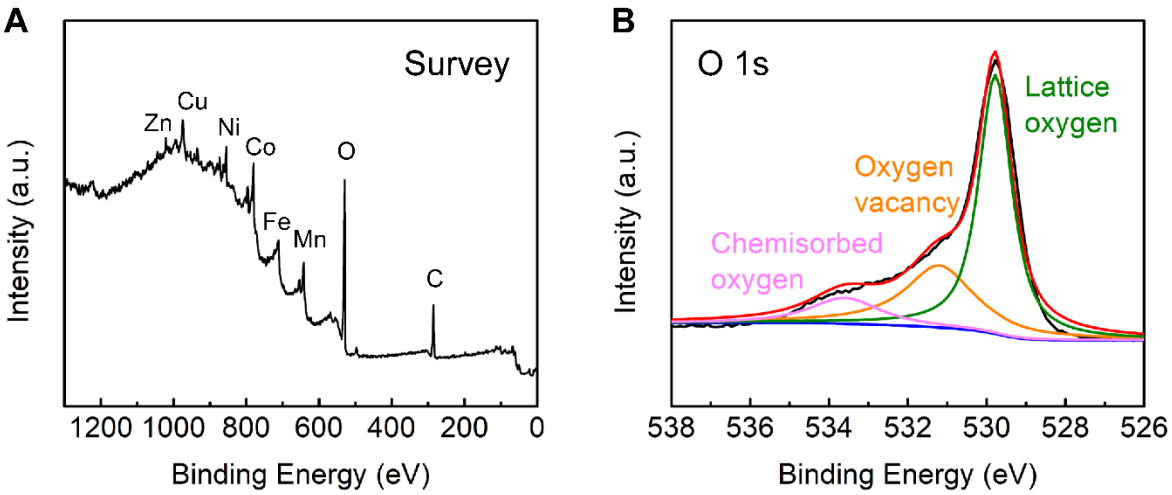

Figure S3. (A) The XPS survey and (B) O 1s spectra of the senary spinel HEO (*i.e.*, $(Mn,Fe,Co,Ni,Cu,Zn)_3O_{4-x}$) synthesized by our high-temperature rapid heating approach.

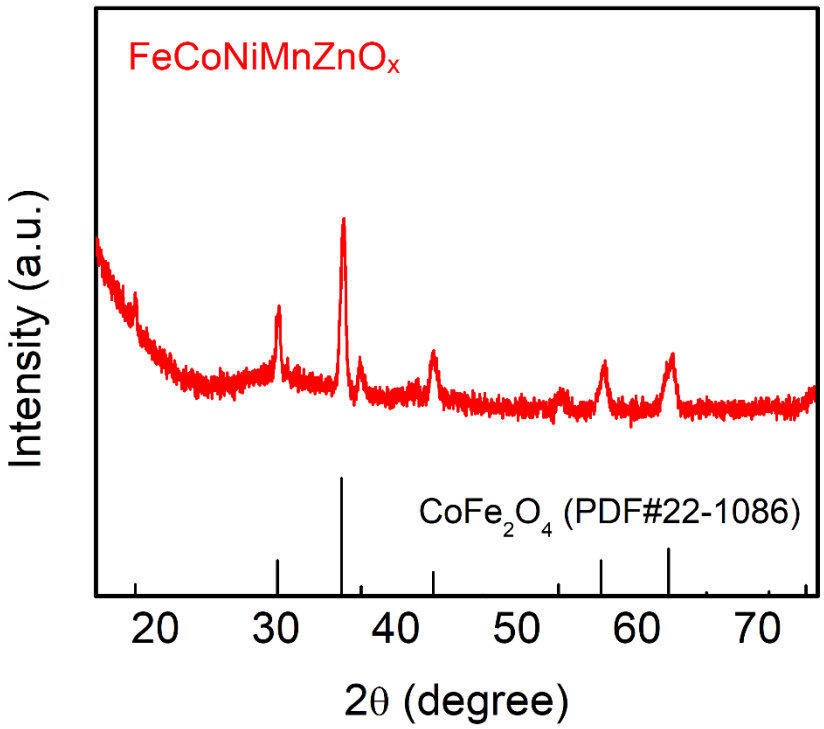

Figure S4. X-ray diffraction pattern of the quinary spinel HEO (*i.e.*, $(Mn,Fe,Co,Ni,Zn)_3O_{4-x}$) synthesized by our high-temperature rapid heating approach. The diffraction pattern agrees well with a typical spinel structure of $CoFe_2O_4$ (PDF#22-1086).

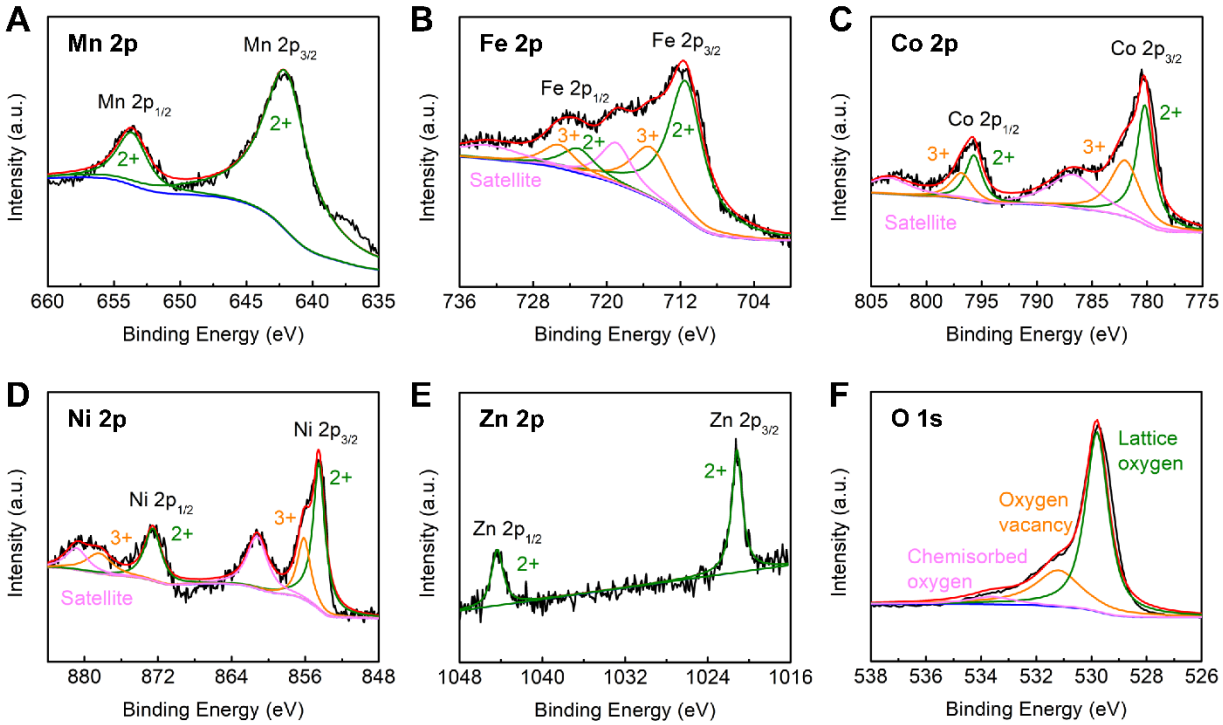

Figure S5. XPS characterization of the quinary spinel HEO (*i.e.*, $(Mn,Fe,Co,Ni,Zn)_3O_{4-x}$) synthesized by the high-temperature rapid heating approach, including the (A) Mn 2p, (B) Fe 2p, (C) Co 2p, (D) Ni 2p, (E) Zn 2p, and (F) O 1s spectra.

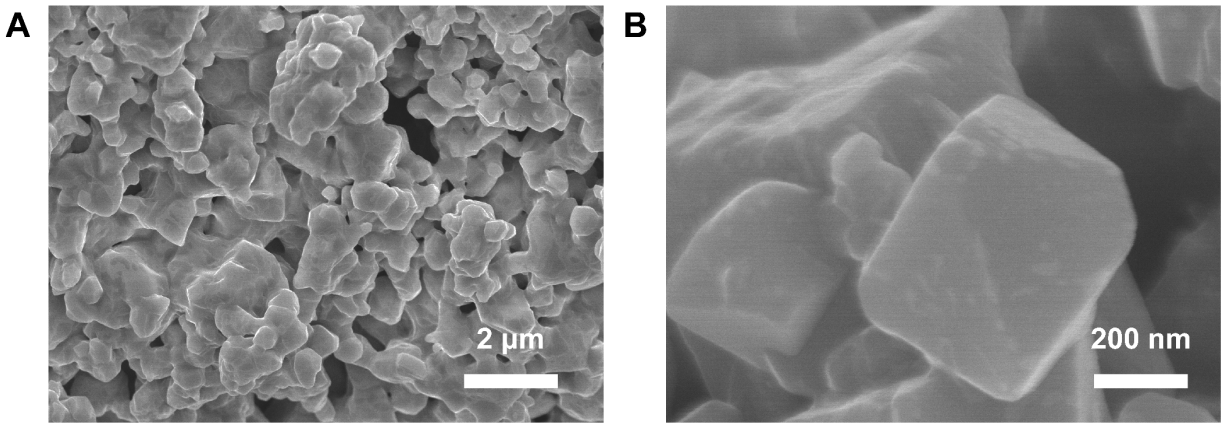

Figure S6. SEM images at (A) low and (B) high magnification of the quinary spinel HEO (*i.e.*, $(Mn,Fe,Co,Ni,Zn)_3O_{4-x}$) synthesized by our high-temperature rapid heating approach.

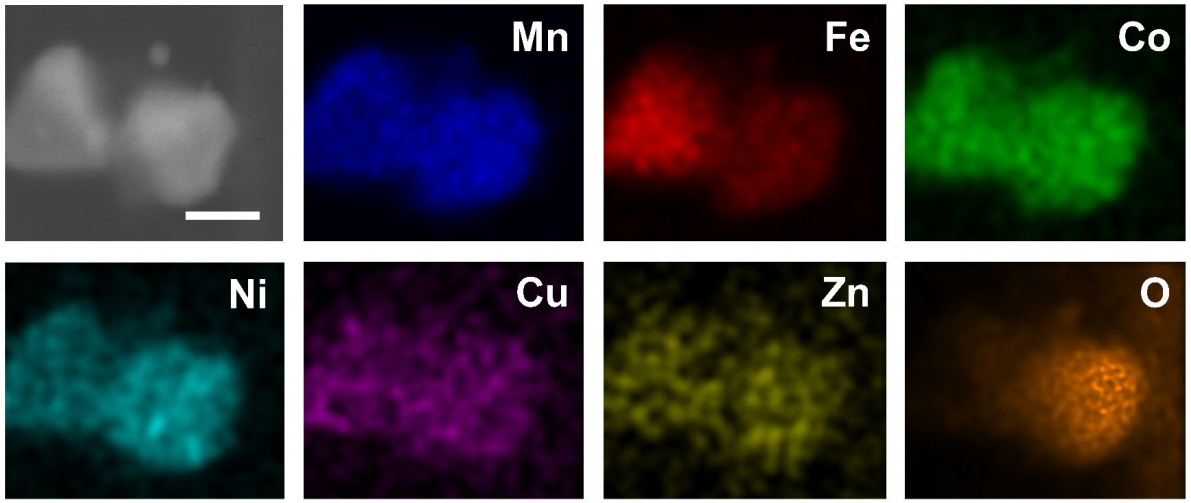

Figure S7. SEM-EDX elemental maps of two senary oxide microparticles (*i.e.*, $(Mn,Fe,Co,Ni,Cu,Zn)_3O_{4-x}$) synthesized by conventional furnace heating (Scale bar: 500 nm). Some parts of the particles show elemental segregation and inhomogeneous distribution. For example, the particle on the left is rich in Fe, while the particle on the right is rich in Ni.

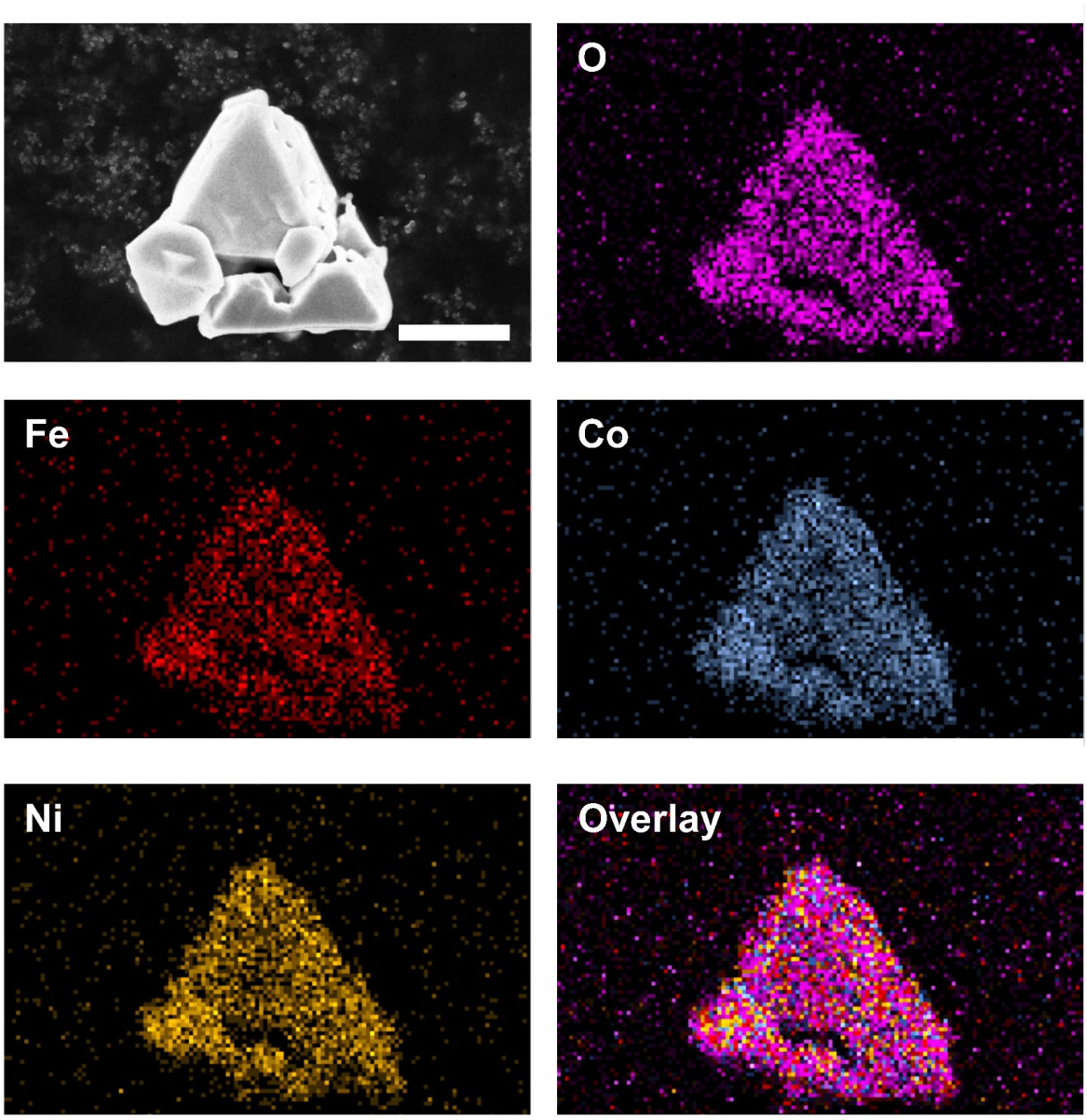

Figure S8. SEM-EDX elemental mapping of the ternary multi-elemental oxide (*i.e.*, Fe, Co, Ni) synthesized by our high-temperature rapid heating approach (Scale bar: 2 μm).

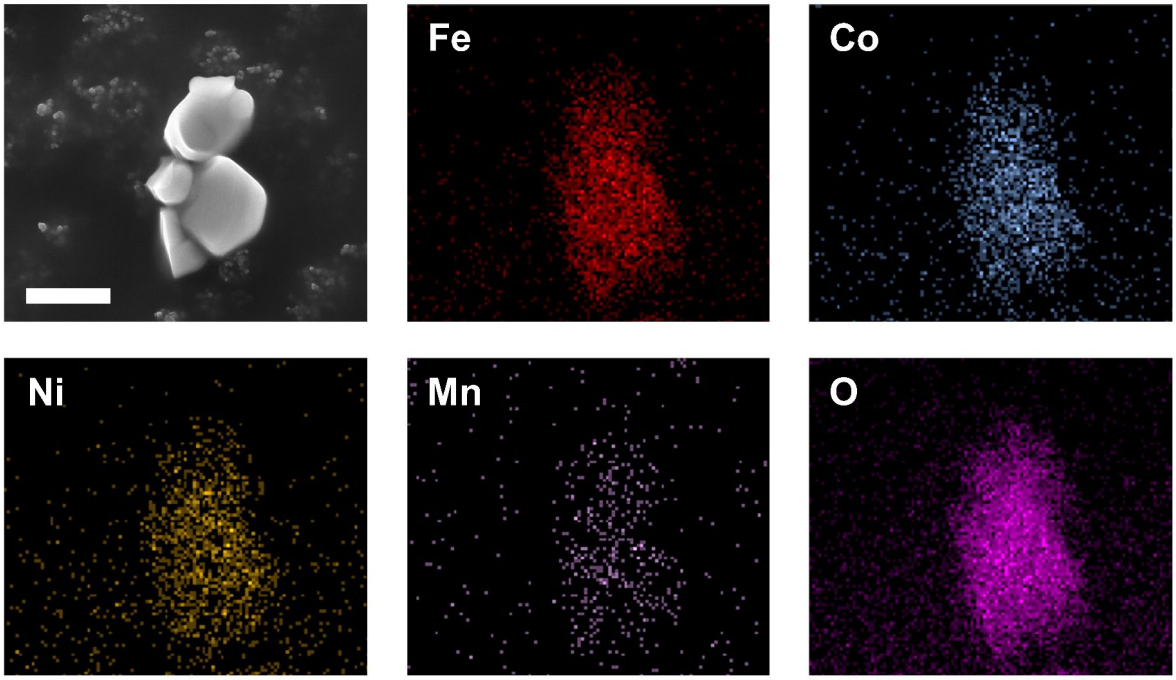

Figure S9. SEM-EDX elemental mapping of the quaternary multi-elemental oxide (*i.e.*, Fe, Co, Ni, Mn) synthesized by our high-temperature rapid heating approach (Scale bar: 1 μm).

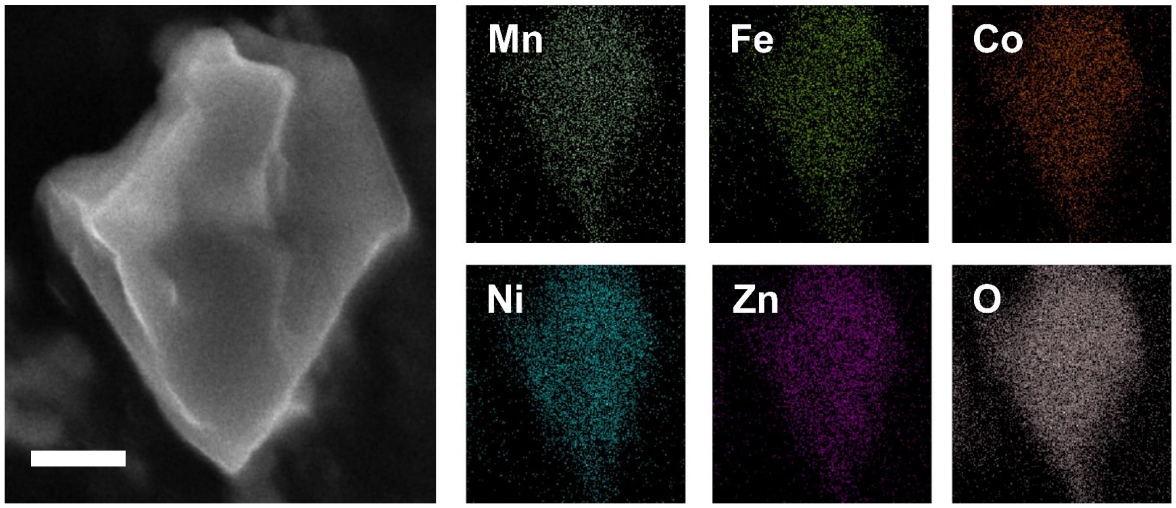

Figure S10. SEM-EDX elemental mapping of the quinary HEO (*i.e.*, Fe, Co, Ni, Mn, Zn) synthesized by our high-temperature rapid heating approach (Scale bar: 300 nm).

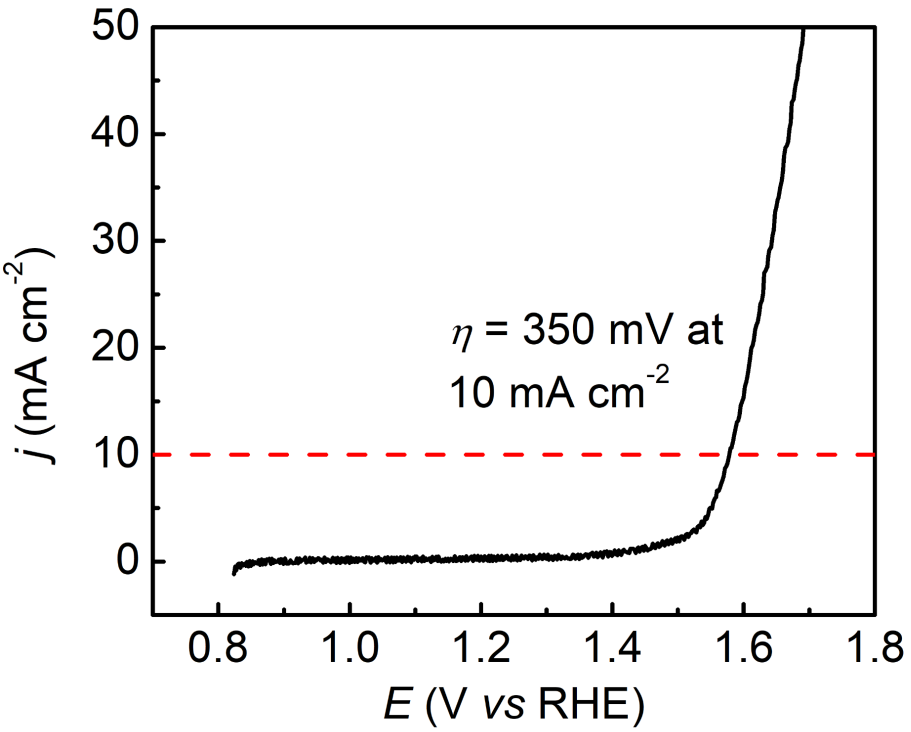

Figure S11. Linear sweep voltammetry of the quinary HEO (*i.e.*, $(Mn,Fe,Co,Ni,Zn)_3O_{4-x}$) synthesized by our high-temperature rapid heating approach (1 mV/s, 1.0 M KOH).

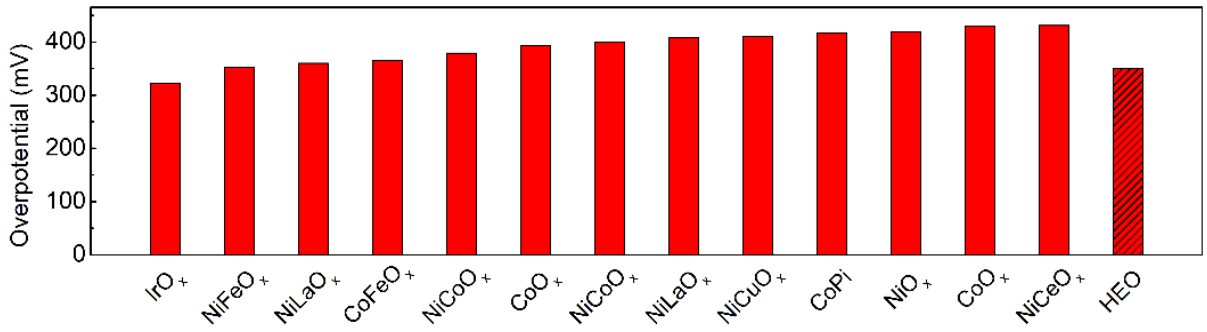

Figure S12. Comparison of the quinary HEO (*i.e.*, $(Mn,Fe,Co,Ni,Zn)_3O_{4-x}$) synthesized by our high-temperature rapid heating approach with benchmarked heterogeneous electrocatalysts. The overpotentials of the benchmarked heterogeneous electrocatalysts are reprinted from literature.[5,6]

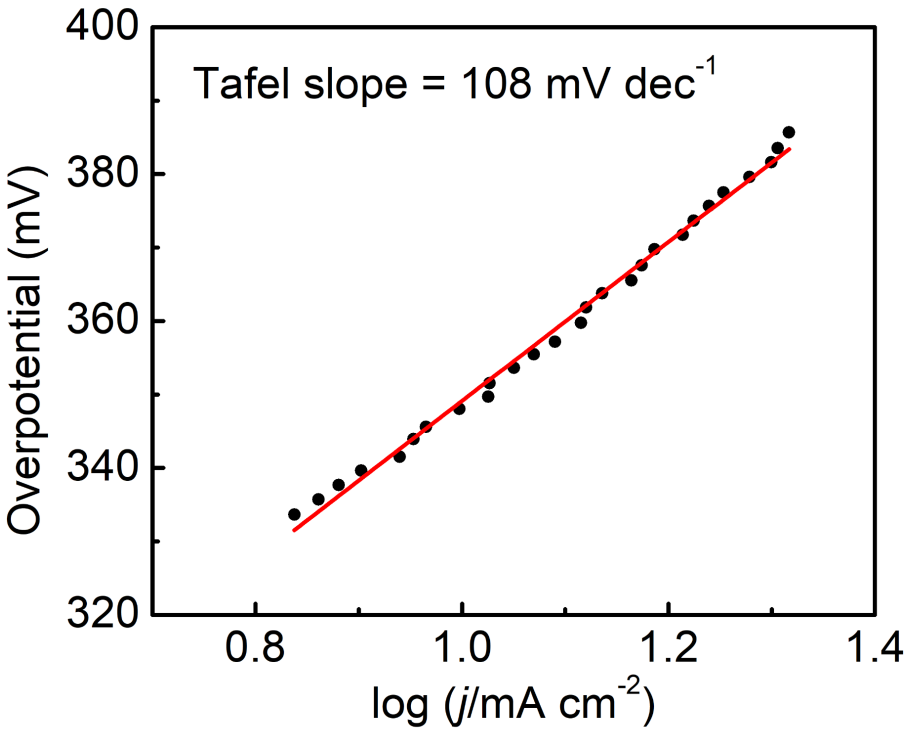

Figure S13. Tafel analysis of the quinary HEO (*i.e.*, $(Mn,Fe,Co,Ni,Zn)_3O_{4-x}$) synthesized by our high-temperature rapid heating approach (1.0 M KOH solution).

Table S1. Comparison of the HEO anodes synthesized by various methods.

Sample	Method	Crystal structure	Capacity mAh/g (Current mA/g)	Cycle numbers	Rate mAh/g (Current mA/g)	Ref.
$(MgTiZnCuFe)O_x$	Solid state reaction and high-energy milling	Spinel	504 (100)	300	272 (2000)	7
$(FeNiCrMnZn)O_x$	Ball-milling and calcination	Hexagonal	387 (500)	185	260 (3000)	8
$(FeCoNiCrMn)O_x$	Hydrothermal	Spinel	800 (500)	200	450 (2000)	9
$(CoCuMgNiZn)O_x$	Nebulized spray pyrolysis	Rock-salt	600 (200)	300	153 (3000)	10
$(NiCoMnFeTi)O_x$	Solid-state sintering	Spinel	560 (100)	100	343 (2500)	11
$(MgCoNiCuZn)O_x$	Solid-state reaction	Rock-salt	600 (89)	60	300 (1800)	12
$(FeCoNiCrMnZnLi)O_x$	Ball-milling and calcination	Spinel	522 (500)	100	173 (2000)	13
$(MgCoNiCuZn)O_x$	Milling and sintering	Rock-salt	475 (100)	100	190 (3000)	14
$(FeCoNiCrMn)O_x$	Solid-state reaction	Spinel	300 (500)	300	182 (2000)	15
$(MnFeCoNiCuZn)O_x$	**High-temperature rapid heating**	**Spinel**	**600 (130)**	**100**	**300 (1600)**	**This work**

Reference

1. T. Fu *et al.*, *J. Heat Transfer* **2010**, *132*, 51602.
2. R. J. Jacob *et al.*, *J. Appl. Phys.* **2018**, *123*, 115902.
3. X. Wang *et al.*, *Mater. Today* **2020**, *35*, 106.
4. T. Li *et al. Nat. Catal.* **2021**, *4*, 62.
5. C. McCrory *et al. J. Am. Chem. Soc.* **2013**, *135*, 16977.
6. C. McCrory *et al. J. Am. Chem. Soc.* **2015**, *137*, 4347.
7. H. Chen *et al. RSC Adv.* **2020**, *10*, 9736.
8. B. Xiao *et al. Ceram. Int.* **2021**, doi.org/10.1016/j.ceramint.2021.08.303.
9. C.-Y. Huang *et al. Chem. Eng. J.* **2021**, *420*, 129838.
10. A. Sarkar *et al. Nat. Commun.* **2018**, *9*, 3400.
11. T. Chen *et al. J. Mater. Chem. A* **2020**, *8*, 21756.
12. P. Ghigna *et al. ACS Appl. Mater. Interfaces* **2020**, *12*, 50344.
13. C. Duan *et al. Ceram. Int.* **2021**, *47*, 32025.
14. S. Wang *et al. Mater. Chem. Phys.* **2021**, *274*, 125105.
15. D. Wang *et al. J. Alloys. Compd.* **2020**, *844*, 156158.